HHS Public Access

Author manuscript

Proc SPIE Int Soc Opt Eng. Author manuscript; available in PMC 2015 December 23.

Published in final edited form as:

Proc SPIE Int Soc Opt Eng. 2015 February ; 9414: . doi:10.1117/12.2082226.

Diagnostic index of 3D osteoarthritic changes in TMJ condylar morphology

Liliane R. Gomes[a,d], **Marcelo Gomes**[b], **Bryan Jung**[c], **Beatriz Paniagua**[c], **Antonio C. Ruellas**[a], **João Roberto Gonçalves**[d], **Martin A. Styner**[c], **Larry Wolford**[e], and **Lucia Cevidanes**[a]

[a]University of Michigan, 1011 North University Avenue, Ann Arbor, MI, USA 48109

[b]Private practice, Salvador, BA, BR, 41940-455

[c]University of North Carolina, 101 Manning Drive, Chapel Hill, NC, USA, 27599

[d]UNESP Univ Estadual Paulista, 1680 Humaita Street, Centro, Araraquara, SP, BR, 14801-903

[e]Baylor University Medical Center, 3501 Junius Street, Dallas, TX, USA, 75246

Abstract

The aim of this study was to investigate imaging statistical approaches for classifying 3D osteoarthritic morphological variations among 169 Temporomandibular Joint (TMJ) condyles. Cone beam Computed Tomography (CBCT) scans were acquired from 69 patients with long-term TMJ Osteoarthritis (OA) (39.1 ± 15.7 years), 15 patients at initial diagnosis of OA (44.9 ± 14.8 years) and 7 healthy controls (43 ± 12.4 years). 3D surface models of the condyles were constructed and Shape Correspondence was used to establish correspondent points on each model. The statistical framework included a multivariate analysis of covariance (MANCOVA) and Direction-Projection- Permutation (DiProPerm) for testing statistical significance of the differences between healthy control and the OA group determined by clinical and radiographic diagnoses. Unsupervised classification using hierarchical agglomerative clustering (HAC) was then conducted. Condylar morphology in OA and healthy subjects varied widely. Compared with healthy controls, OA average condyle was statistically significantly smaller in all dimensions except its anterior surface. Significant flattening of the lateral pole was noticed at initial diagnosis ($p < 0.05$). It was observed areas of 3.88 mm bone resorption at the superior surface and 3.10 mm bone apposition at the anterior aspect of the long-term OA average model. 1000 permutation statistics of DiProPerm supported a significant difference between the healthy control group and OA group ($t = 6.7$, empirical p-value = 0.001). Clinically meaningful unsupervised classification of TMJ condylar morphology determined a preliminary diagnostic index of 3D osteoarthritic changes, which may be the first step towards a more targeted diagnosis of this condition.

CONFLICT OF INTEREST STATEMENT

This is an original work that has not been, submitted for publication or presentation elsewhere. All authors had no financial and personal relationships with other people or organizations that could inappropriately influence (bias) their work.

Keywords

Temporomandibular Joint Disorders; Osteoarthritis; Bone Resorption; Bone Overgrowth; 3D imaging

1. INTRODUCTION

TMJ's osteoarthritis has been described as a progressive degenerative joint disorder caused by a pathological imbalance between the dynamic processes of breakdown and repair of the organic tissues.[1–5] The course of the disease challenges experts given the different morphological patterns of progression observed in its various stages.[6] It may evolve into repair and morphological adaptation, featuring a functional remodeling.[7, 8] However, it may present with an adverse course characterized by aggressive bone destruction, deformity of related structures and functional impairment.[2, 6, 7] This unpredictable scenario hampers the development of valid therapies.[3, 9]

The TMJ differs from other joints because it is covered by a layer of fibrocartilage, instead of hyaline cartilage.[9] The bone of the mandibular condyles is located just beneath the fibrocartilage, making it particularly vulnerable to inflammatory damage and a valuable model for studying arthritic bony changes. The bone in the TMJ condyle is the site of numerous dynamic morphological transformations, which are an integral part of the initiation/progression of arthritis, not merely secondary manifestations to cartilage degradation. Thus, a strong rationale exists for therapeutic approaches that target bone resorption and formation.[10–14]

Clinical and pathological presentation of TMJ OA range from mild failure of the joint components with disc displacement and degeneration, to loss of articular fibrocartilage, synovitis, and subchondral bone alterations such as sclerosis, flattening, erosions and bone overgrowth with osteophytes formation.[1, 5, 15] Upon diagnosis of initial signs of active TMJ destruction, it is essential to monitor the disease, either localized to the TMJ or systemic, before loading the joints with orthodontic/orthopedic forces or undertaking jaw surgery.

CBCT has assumed a prominent role in the diagnosis of condylar resorption.[16] It provides a clear visualization of the hard tissues of the TMJ[1, 15, 16] and markedly reduces radiation and cost compared to medical CT.[15] Through the analysis of different tomographic slices it becomes possible to identify specific changes in the anatomy of the mandibular condyles with osteoarthritis. Moreover, new technologies such as the use of 3D surface models allows for a comprehensive evaluation of the overall morphological alterations.

3D shape correspondence analysis (SPHARM-PDM) has aroused the interest of the medical community due to its accuracy in locating and quantifying morphological changes between healthy and pathological structures.[17] This innovative method for diagnosing TMJ osteoarthritis minimizes the importance of examiner's experience, reducing intra- and inter-rater related errors, standardizes findings, allowing new discoveries, and also contributes to the development of new imaging markers for risk factors.[1]

This study objective was to investigate novel imaging statistical approaches to classify 3D osteoarthritic morphological variations, as determined by 1002 bone imaging markers in the TMJ condylar surface. Specifically, this study proposed to identify differences among the asymptomatic controls and the TMJ OA group by means of supervised classification. Then, the unsupervised classification categorized such complex disease, making it possible the development of a preliminary diagnostic index of TMJ condylar osteoarthritis.

2. METHODS

Sixty nine patients with long-term TMJ OA (39.1 ± 15.7 years), 15 patients at initial consult diagnosis of OA (44.9 ± 14.8 years) and 7 healthy controls (43 ± 12.4 years), recruited from the university clinic and through advertisement, underwent a clinical exam by an orofacial pain specialist using diagnostic criteria guidelines. Following clinical diagnosis of TMJ osteoarthritis or health, a 20-second CBCT scan was taken on all participants, using the same machine (i-Cat® CBCT, 120 kV, 18.66 mA, Imaging Sciences, Hatfield, PA) and a large field of view to include both TMJs. The study was approved by the university institutional review board and all subjects consented to the investigation.

3D surface mesh models of the right and left mandibular condyles were constructed by outlining the cortical boundaries of the condylar region using semi-automatic discrimination procedures, that allowed manual editing, checking slice by slice in all three planes of space (ITK-SNAP software v.2.4, www.itksnap.org).[18] After generating all 3D surface models, left condyles were mirrored in the sagittal plane to form right condyles to facilitate comparisons. Twenty-five landmarks were placed on the surface of each condyle by one observer at corresponding (homologous) areas to closely approximate the various anatomic regions of all individuals who present marked morphological variability (Figure 1). The regional superimposition technique used in the present study for across subject comparisons have been validated by Schilling et al.[19] After registration, all condylar models were simultaneously cropped to define the condylar region of interest. SPHARM-PDM software (SPHARM-PDM software, http://www.nitrc.org/projects/spharm-pdm)[20] was used to generate a mesh approximation from the volumes, whose 1002 points were mapped to a sphere. An average 3D condylar shape was generated for the TMJ OA groups and control group (Figure 2A) (Linux MeshMath script, http://www.nitrc.org/projects/spharm-pdm).[20] The core of the ability to compute the group average and group variability is the establishment of correspondence between each of the 1002 points in the condylar surface models across all subjects.

The Linux MeshMath script was then used to calculate 3D point-wise subtractions between each group's average morphology (Figure 2A). Semi-transparent overlays between the average models in 3D Slicer software [21] were used to visually compare the different morphologies (Figure 2B). The computed 1002 vector differences were displayed on the condyle surface, scaled according to the magnitude of the difference and pointing in the direction of the change. The patterns of variation across TMJ OA and control samples were determined through the calculation of signed distances, where the areas of bone resorption were displayed as negative values (blue), no differences (0 mm surface distances, white) or bone proliferation as positive (red) (Figure 3A).

The statistical framework for testing morphological variations of the 169 condyles included supervised and unsupervised classifications. A Hotelling T^2 test, in a multivariate analysis of covariance (Shape analysis MANCOVA software)[22] assessed statistically significant morphological variations between the average condyle models. Direction-Projection-Permutation (DiProPerm) was used for testing high dimensional hypotheses. The DiProperm method was aimed at rigorous testing of whether lower dimensional visual differences were statistically significant [23] through three steps: (1) determining Direction by projecting samples onto an appropriate direction; (2) Projection by calculating univariate two sample statistics; and (3) Permutation by assessing significance using 1000 permutations of group membership. Distance Weighted Discrimination (DWD)[24] calculated a direction vector to classify high dimensional datasets, and their principal components (PC) were graphically plotted. Given the fact that the control and OA samples have different sample size, an appropriately weighted version of DWD, the wDWD, was used to find a direction vector in the feature space separating the morphology groups. Unsupervised classification using hierarchical agglomerative clustering (HAC) was conducted in order to group unlabelled data into subsets (clusters) that are believed to reflect the underlying structure of the data, based on morphological similarity.

3. RESULTS

Qualitative assessment of the semi-transparent overlays revealed that, even at their initial diagnostic appointment, OA patients already presented with noticeable morphological bone changes that were more marked in the group with long-term history of TMJ osteoarthritis (Figure 2B). Quantitative assessment of group comparisons were reported using signed distance maps computed locally at each correspondent point. Compared to the healthy control group, the long-term OA average model was of smaller size in all dimensions except its anterior surface, and areas of statistically significant differences were observed along the whole condylar surface except at the pterygoid fossa and part of the lateral aspect of the condylar neck ($p < 0.05$). Considering the comparison between the healthy control and initial diagnosis average models, areas of statistically significant differences were noticed in the superior articular surface of the condyles, particularly in the anterior and superior portions of the lateral pole and also in the medial pole and medial aspect of the condylar neck ($p < 0.05$). Areas indicating 2.38 mm bone resorption were observed at the superior surface of the initial diagnosis average model and 3.88 mm in the long-term group as compared to the healthy control group. In the anterior surface of the condyle, a small area of 1.86 mm of bone apposition was noted at initial diagnosis and 3.10 mm at the long-term OA average models compared to healthy controls. When the initial diagnosis and long term OA average models were compared, statistically significant differences indicative of disease progression were also noticed ($p < 0.05$). It was observed an area of 1.98 mm bone apposition at the anterior surface and 2.64 mm bone resorption at the superior articular surface of the long-term OA average model (Figure 3).

Regarding the supervised classification, DiProPerm test found a statistically significant morphological difference between the healthy control and the OA group (p-value = 0.001). The projected plots of the healthy control condyles tended to cluster and were clearly separated from the OA groups. Most projected plots of initial diagnosis condyles were

located within the bounds of the plots of the long-term diagnosis condyles. The maximal partition of condylar morphology, as established by 1002 points in each individual condyle, was observed in the graphic plots of the principal component refined in the wDWD direction. The wDWD direction onto the PC was shown by the angle in the PC analysis score plots (Figure 4). The maximum variability in this cohort (both OA and Healthy) occurred in condylar head morphology as a whole (PC1), then in the medial pole (PC2) and in the lateral pole (PC3). The projections in the wDWD direction indicated the characteristic condylar remodeling from healthy condyles to OA groups.

Clinically meaningful unsupervised classification of condylar morphology was obtained using hierarchical agglomerative clustering (HAC). A detailed cluster dendogram classified individual condyles to subgroups that identified distinct condylar morphologies (Figures 5). The y-axis of the dendogram is a measure of closeness (i.e. linkage criterion) of linked clusters. The lower linked cluster means that those condyles were morphologically similar as compared to condyles in the next upper cluster or other clusters. The height on the y-axis is a distance between connected groups to the next higher cluster. Thus, greater height difference means more morphological difference between clusters. The x-axis shows a metric (a measure of distance between pairs of observations) and a Euclidean distance that was used to calculate the distance between pairs. Along with the x-axis, clusters with the most similarity are lined up from left to right: a cluster on the very left side will be most different than a cluster on the very right side. In Figure 5, we can see in the detail the condyles that were the most dissimilar. Figure 6 illustrates all the 169 condyles superimposed on the average control following the same sequence exhibited in the dendogram.

4. NEW OR BREAKTHROUGH WORK TO BE PRESENTED

These novel statistical approaches revealed imaging biomarkers of the bone resorption and repair at the articular surfaces of the condyle. Even tough the ability to predict progression is not properly addressable in the cross-sectional study design, these biomarkers can be reasonable surrogate biomarkers of tissue destruction and/or repair overtime. Unsupervised classification provided a preliminary diagnostic index of 3D osteoarthritic changes in TMJ condylar morphology, which may be the first step towards a more targeted diagnosis of this condition. As we continue to increase the control and OA sample sizes, future studies may allow statistical description of combinatorial biomarker assessments such as receiver operating characteristic (ROC) curves on disease versus health, as well as classification-based schemes for computer-aided diagnosis of TMJ OA.

ACKNOWLEDGMENTS

This work was supported by the National Institute of Dental & Craniofacial Research of the National Institutes of Health under Award Number R01DE024450 and by the Sao Paulo Research Foundation (FAPESP, Brazil, Grant 2013/22417-0). The content is solely the responsibility of the authors and does not necessarily represent the official views of the National Institutes of Health.

REFERENCES

1. Cevidanes LH, Hajati AK, Paniagua B, Lim PF, Walker DG, Palconet G, Nackley AG, Styner M, Ludlow JB, Zhu H, Phillips C. Quantification of condylar resorption in temporomandibular joint osteoarthritis. Oral Surg Oral Med Oral Pathol Oral Radiol Endod. 2010; 110:110–117. [PubMed: 20382043]
2. Tanaka E, Detamore MS, Mercuri LG. Degenerative disorders of the temporomandibular joint: etiology, diagnosis, and treatment. J Dent Res. 2008; 87(4):296–307. [PubMed: 18362309]
3. Hunter DJ, Hellio Le Graverand-Gastineau MP. How close are we to having structure-modifying drugs available? Med Clin North Am. 2009; 93(1):223–234. [PubMed: 19059031]
4. Rousseau JC, Delmas PD. Biological markers in osteoarthritis. Nature Clinical Practice Rheumatology. 2007; 3(6):346–356.
5. van Spil WE, DeGroot J, Lems WF, Oostveen JC, Lafeber FP. Serum and urinary biochemical markers for knee and hip-osteoarthritis: A systematic review applying the consensus BIPED criteria. Osteoarthritis and Cartilage/ OARS, Osteoarthritis Research Society. 2010; 18(5):605–612.
6. Samuels J, Krasnokutsky S, Abramson SB. Osteoarthritis: A tale of three tissues. Bulletin of the NYU Hospital for Joint Diseases. 2008; 66(3):244–250. [PubMed: 18937640]
7. Arnett GW, Milam SB, Gottesman L. Progressive mandibular retrusion-idiopathic condylar resorption. Part II. Am J Orthod Dentofacial Orthop. 1996; 110(2):117–127. [PubMed: 8760837]
8. Bland JH. The reversibility of osteoarthritis: a review. Am J Med. 1983; 74(6A):16–26. [PubMed: 6344622]
9. Wadhwa S, Kapila S. TMJ disorders: Future innovations in diagnostics and therapeutics. Journal of Dental Education. 2008; 72:930–947. [PubMed: 18676802]
10. Abramson SB, Attur M. Developments in the scientific understanding of osteoarthritis. Arthritis Res Ther. 2009; 11:227. [PubMed: 19519925]
11. Bauer DC, Hunter DJ, Abramson SB, Attur M, Corr M, Felson D, Heinegård D, Jordan JM, Kepler TB, Lane NE, Saxne T, Tyree B, Kraus VB. Classification of osteoarthritis biomarkers: A proposed approach. Osteoarthritis and Cartilage. 2006; 14:723–727. [PubMed: 16733093]
12. Hayami T, Pickarski M, Wesolowski GA, McLane J, Bone A, Destefano J, Rodan GA, Duong le T. The role of subchondral bone remodeling in osteoarthritis: reduction of cartilage degeneration and prevention of osteophyte formation by alendronate in the rat anterior cruciate ligament transection model. Arthritis Rheum. 2004; 50:1193–1206. [PubMed: 15077302]
13. Hunter DJ, Eckstein F, EKraus VB, Losina E, Sandel L, Guermazi A. Imaging Biomarker Validation and Qualification Report. Sixth OARSI Workshop on Imaging in Osteoarthritis combined with Third OA. Biomarkers Workshop. Osteoarthritis and Cartilage. 2013; 21:939e942. [PubMed: 23639411]
14. Karsdal MA, Martin TJ, Bollerslev J, Christiansen C, Henriksen K. Are nonresorbing osteoclasts sources of bone anabolic activity? J Bone Miner Res. 2007; 22:487–494. [PubMed: 17227224]
15. Alexiou K, Stamatakis H, Tsiklakis K. Evaluation of the severity of temporomandibular joint osteoarthritic changes related to age using cone beam computed tomography. Dento Maxillo Facial Radiology. 2009; 38(3):141–147. [PubMed: 19225084]
16. Ahmad M. Research diagnostic criteria for temporomandibular disorders (RDC/TMD): Development of image analysis criteria and examiner reliability for image analysis. Oral Surgery, Oral Medicine, Oral Pathology, Oral Radiology and Endodontics. 2009; 107(6):844–860.
17. Paniagua B, Cevidanes LHS, Walker D, Zhu H, Guo R, Styner M. Clinical application of SPHARM-PDM to quantify temporomandibular joint osteoarthritis. Computerized Medical Imaging and Graphics. 2011; 35:345–352. [PubMed: 21185694]
18. Itksnap.org. Penn Image Computing and Science Laboratory. Philapelphia: University of Pennsylvania; 2013 Apr 17. <http://www.itksnap.org> (15 October 2013) www.itksnap.org/pmwiki/pmwiki.php?n=Main.Downloads.
19. Schilling J, Gomes LR, Benavides E, Nguyen T, Paniagua B, Styner M, Boen V, Gonçalves JR, Cevidanes LH. Regional 3D superimposition to assess temporomandibular joint condylar morphology. Dentomaxillofac Radiol. 2014; 43(1):20130273. [PubMed: 24170802]

20. Neuroimaging Informatics Tools and Resources Clearinghouse (NITRC.org). Projects Spharm-PDM. Chapel Hill: Neuro Image Research and Analysis Laboratories, University of North Carolina; 2013 Jul 21. <http://www.NITRC.org> (22 July 2013). www.nitrc.org/projects/spharm-pdm

21. Slicer.org. Surgical Planning Laboratory. Boston: Harvard Medical School; <http://slicer.org> (01 Sep 2014). www.download.slicer.org

22. Neuroimaging Informatics Tools and Resources Clearinghouse (NITRC.org). Projects Shape Analysis Mancova. Chapel Hill: Neuro Image Research and Analysis Laboratories, University of North Carolina; 2013 Jun 27. <http://www.NITRC.org> (15 October 2013). www.nitrc.org/projects/shape_mancova

23. Wei, S. Latent supervised learning and DiProPerm. Chapel Hill: The University of North Carolina; 2014.

24. Qiao X, Zhang HH, Liu Y, Todd MJ, Marron JS. Weighted Distance Weighted Discrimination and its Asymptotic Properties. Journal of the American Statistical Association. 2009; 105(489):401–414. [PubMed: 21152360]

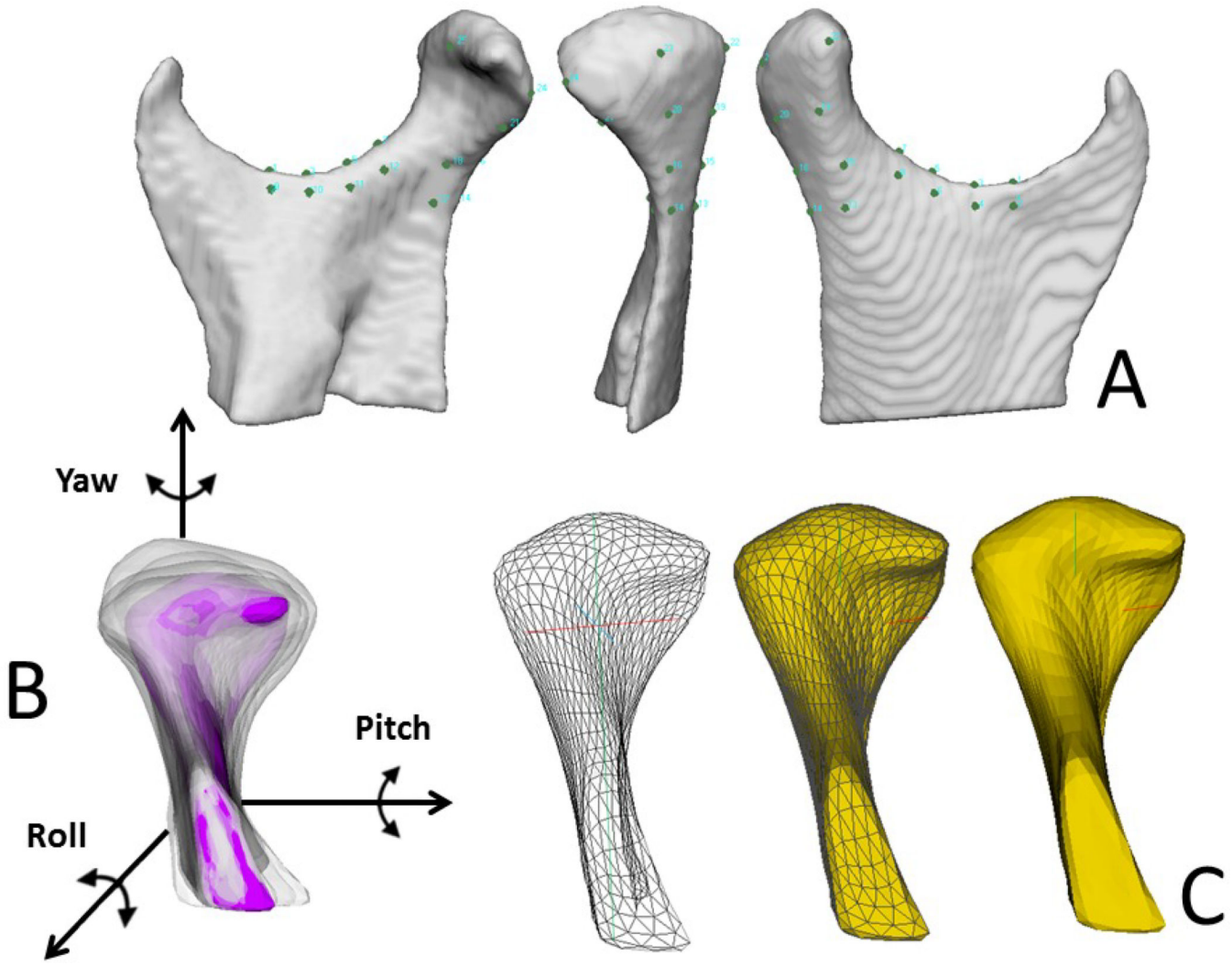

Figure 1.

A. 25 points in the ramus and condyle surfaces used for the landmark-based registration, B. Reference condylar model (purple) with the overlay of multiple condyles approximated in the same coordinate system, C- Parameterization of 1002 correspondent surface mesh points for statistical comparisons and detailed morphological characterization.

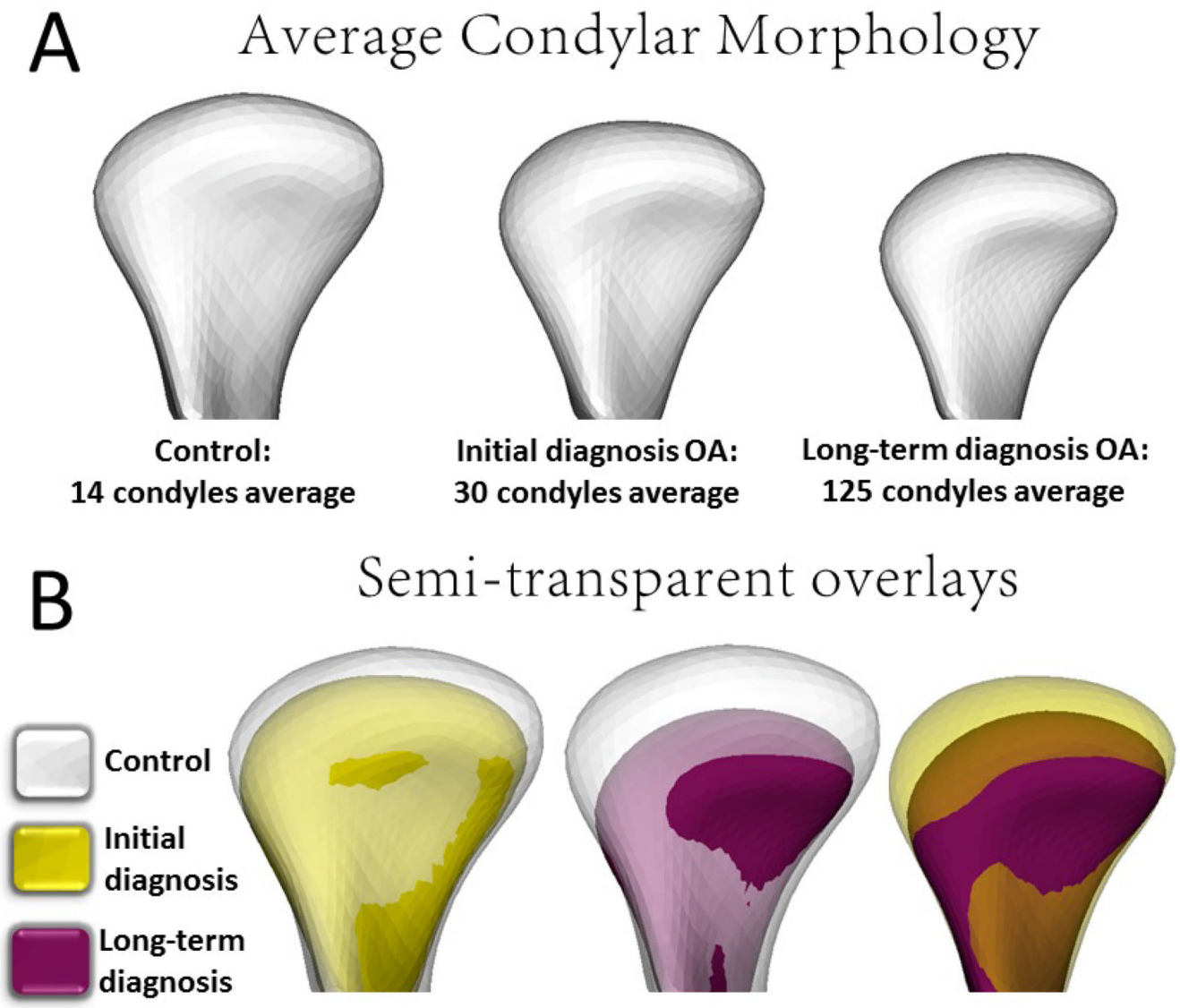

Figure 2.

A. Average condylar morphology. B. Semi-transparent overlays of group average morphologies. At their initial diagnostic appointment OA patients already presented marked bone changes that are more severe in the group with long-term OA.

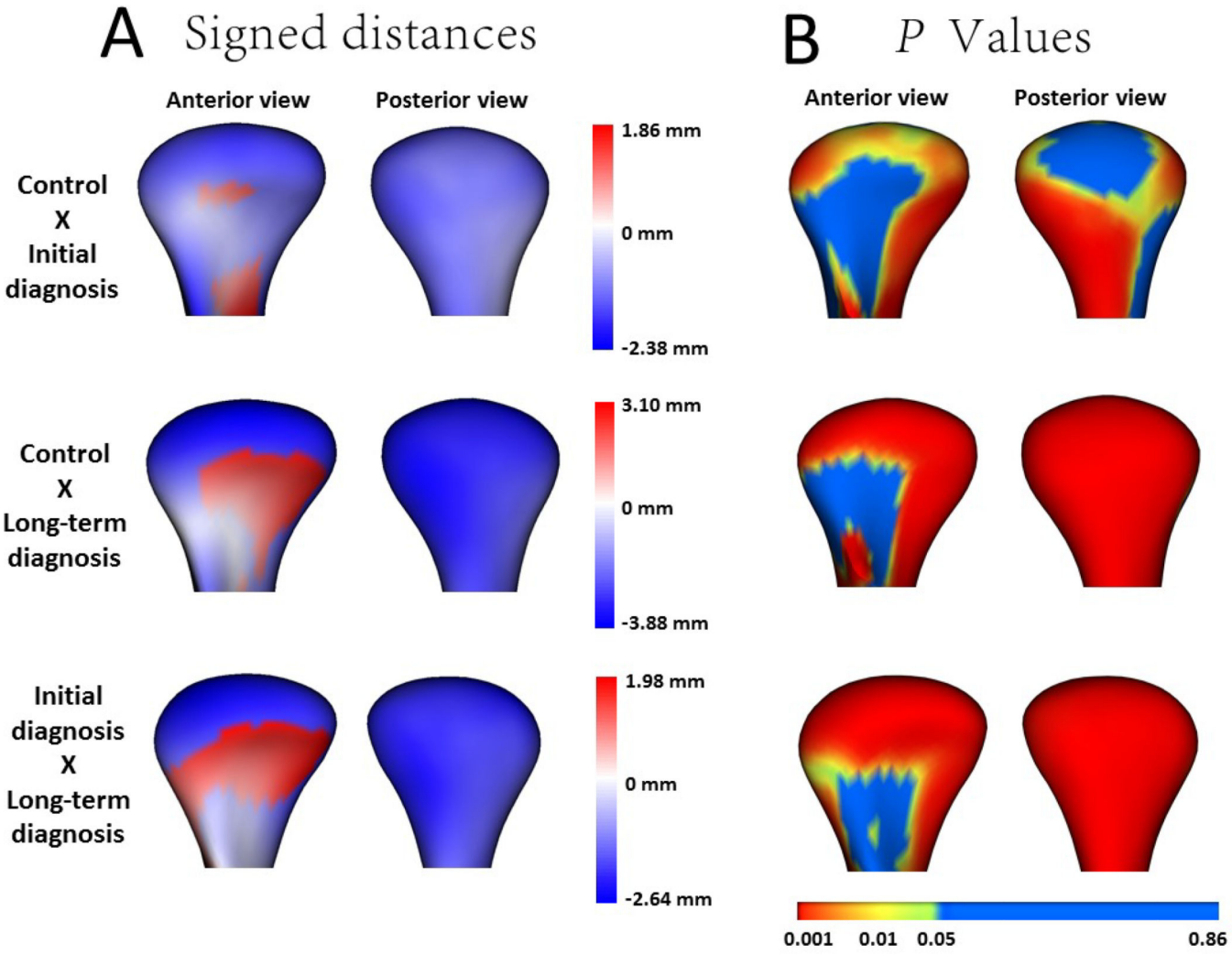

Figure 3.

A. Quantitative assessment of condylar morphology is shown in signed distance color-coded maps computed locally at each correspondent surface point: blue areas are indicative of bone resorption and red areas are indicative of bone overgrowth. B. In the *P* value map, highly significant differences ($p < 0.01$) are color-coded with red, intermediate significant differences are color-coded with green ($0.01 > p > 0.05$) and non-significant differences are color-coded with blue ($p > 0.05$).

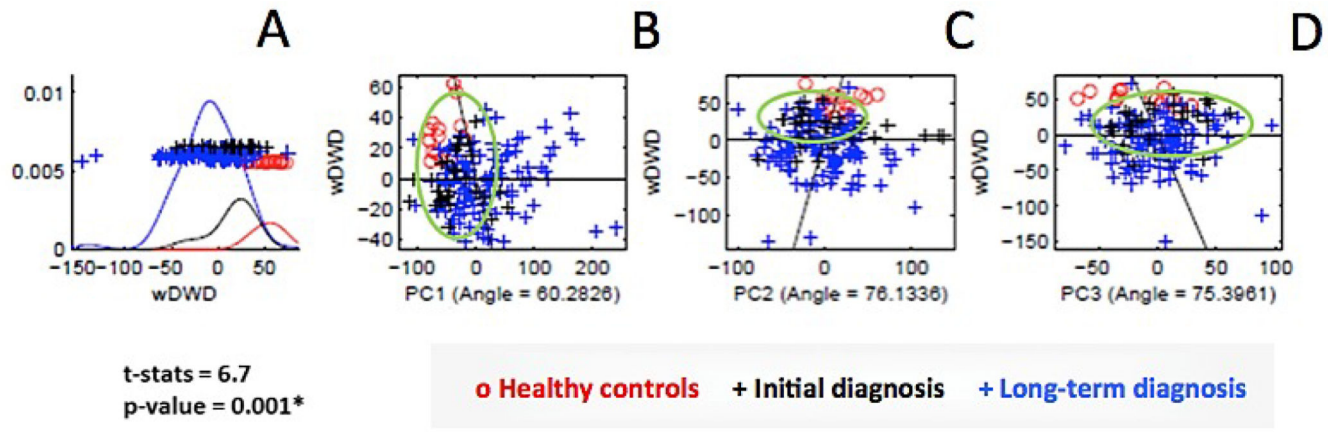

Figure 4.

DiProPerm graphic results. The left panel shows the distribution of the data projected onto the wDWD direction, illustrating how well the groups can be separated. The curves in the left panel are smooth histograms, with each color showing the sub-histograms for the different groups. The center and right panels show principal component graphics, where each condyle is plotted in the first, second and third principal direction. The horizontal x-axis is the projected value, and the vertical y-axis reflects order in the data set, to avoid overplotting. A. wDWD shows the direction that represents the best dissociation among the three classes. This classification includes non-uniform, complex condylar head surface modeling, as well as neck torque, overall condylar morphological variability, considering both the lateral and medial poles. B. PC1 shows general condylar morphological variability in the wDWD direction. C. PC2 shows medial pole morphological variability in the wDWD direction. D. PC3 reports lateral pole morphological variability in the wDWD direction.

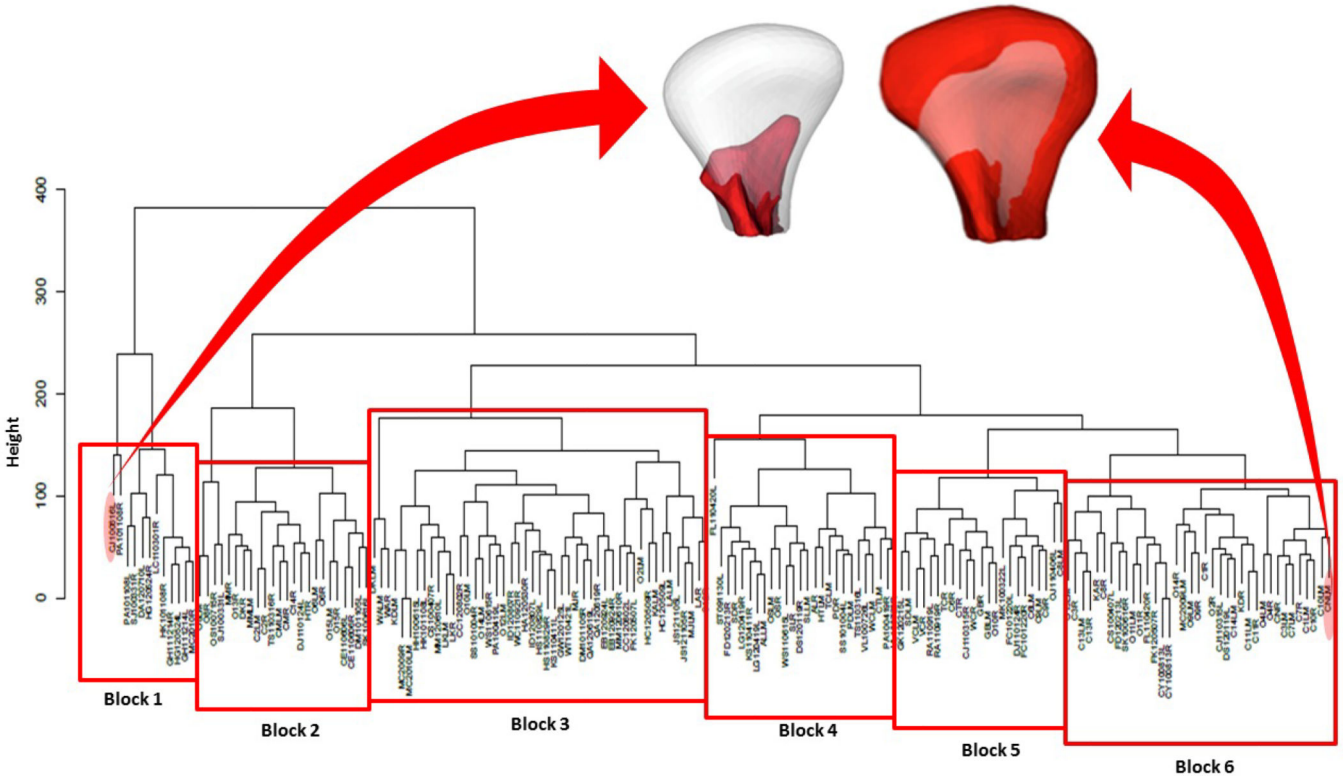

Figure 5.
Cluster Dendogram with a complete-linkage method of all 169 condyles. Note in the detail the greatest different condyles (red) superimposed on the same average control (white) for comparison.

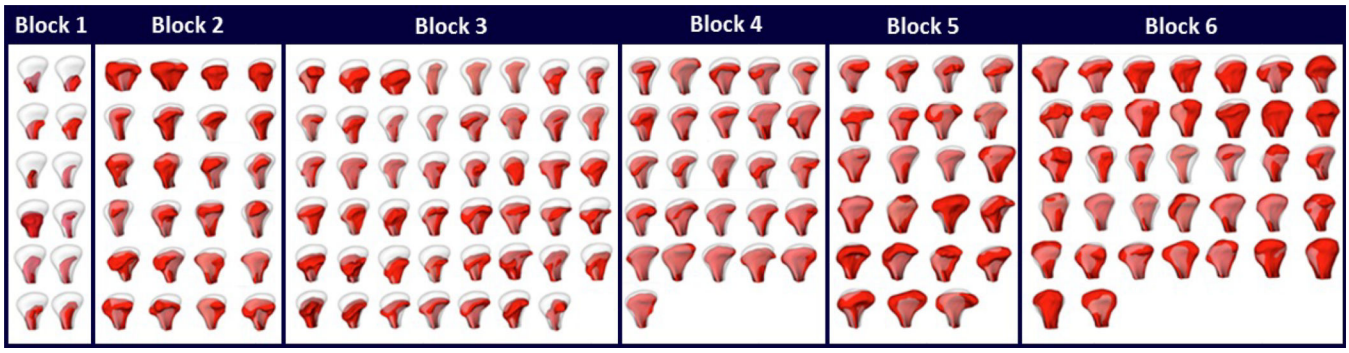

Figure 6.
The whole sample (169 condyles) divided into 6 blocks according to the unsupervised classification. All condyles (red) were superimposed on the same average control (white).